

Changes Made on a 2.7-m Long Superconducting Solenoid Magnet Cryogenic System that allowed the Magnet to be kept cold using 4 K Pulse Tube Coolers

M. A. Green^a, H. Pan^a, and R. M. Preece^b

^aLawrence Berkeley Laboratory, Berkeley CA 94720, USA

^bSTFC Rutherford Appleton Laboratory, Didcot, Oxfordshire, UK

Abstract. Two 2.7-m long solenoid magnets with a cold mass of 1400 kg were fabricated in between 2007 and 2010. The magnet cryostat outside diameter is ~1.4 meters and the cryostat length is ~2.73 meters. The magnet warm bore is 0.4 meters. The magnet was designed to be cooled using three 1.5 W two-stage coolers. In both magnets, three coolers could not keep the cryostat filled with liquid helium. The temperatures of the shield and the tops of the HTS leads were too warm. A 140 W single stage cooler was added to magnet 2 to cool the HTS leads, the shield and the cold mass support intercepts. When the magnet 2 was retested in 2010, the net cooling at 4.2 K was -1.5 W with first-stage temperatures of the four coolers at ~42 K. The tops of the HTS leads were <50 K, but the shield and cold mass support intercepts remained too warm. The solenoid cryostat and shield were modified during 2011 and 2012 to reduce the 4.2 K heat load and increase the cooling. This magnet was tested in 2012, with five 1.5 W two-stage coolers and the single stage cooler. The changes made in the magnet are described in this report. As a result of the cryostat and shield changes, and adding 3.0 W of cooling at 4.2 K, the net 4.2 K cooling changed from -1.6 W to +5.0 W. About half of the change in net cooling to this magnet was due changes that reduced the shield temperature. This report demonstrates the importance of running the shield cold (~40 K) and reducing the heat loads from all sources on both the shield and the cold mass.

Keywords: Superconducting Magnet, 4 K Cooling, 50 K Shield Material, and 50 K Shield Cooling.

PACS: 07.20.Mc, 84.71.Ba

THE MAGNET AND CRYOSTAT PARAMETERS AS ORIGINALLY BUILT

A pair of 2.7-m long superconducting solenoids were fabricated between 2007 and 2009. These solenoids were designed to produce a uniform solenoidal magnetic field ($\Delta B/B < 0.003$) within 0.4-m diameter warm bore. The good field region is 1.0-m long and 0.3-m in diameter [1]. This uniform field region is occupied by five planes of scintillating fiber detector that measure the position in 3D space of π^+ , π^- , μ^+ , μ^- , e^+ and e^- as they spiral around in the solenoid field. The uniform field in the range from 2.8 to 4.0 T (both polarities) is generated by a 1.3-m long center solenoid with two 0.06-m long end coils that shape the field [2]. The uniform field section is matched to the rest of the experiment by two coils that match to two-coil solenoid that can produce a maximum B of 2.5 T (both polarities) on axis. The two-coil magnet that is matched to the uniform field solenoid may also produce a cusp shaped field that is zero in the center of the magnet with a maximum B of ± 3.5 T on axis [3].

The uniform field section has the two end coils and the center coil powered from a single 300-A power supply. The end coil currents can be varied by ± 60 A with separate power supplies. The two match coils are separately powered using 300-A power supplies. The maximum current in all operating modes for the magnet is expected to be 275 A. The magnet is supplied with current by six commercial HTS leads rated at 500 A and two commercial HTS leads rated at 100 A. The lead current ratings apply at 64 K in the self-field generated by the leads [4].

TABLE 1 shows the five-coil detector solenoid parameters for magnet 2 at a beam momentum of 240 MeV/c [5]. The currents in magnet 1 are identical to magnet 2 within 0.06 percent. The total stored energy of the magnet at the highest is design currents is >3.5 MJ. The magnet is protected using nine sets of back-to-back diodes and 0.02-ohm resistors. The long coil is sub-divided into two sections. Quench-back greatly speeds up the magnet quench process in the long center coil, because the whole center coil will quench back ~10 s before a quench will propagate from one end of the long coil to the other [6]. In the other coils, quench back isn't very important. A quench from one match coil to another is propagated through thermal diffusion through the aluminum mandrel. The resistors and diodes attached to the center coil play a very important role in protecting the magnet whenever an LTS or an HTS lead fails [7]. The resistor pack was modified to enhance the magnet protection in the event of a lead failure [8].

TABLE 1. Detector magnet 2 parameters as fabricated [5]. The parameters of magnet 1 are within ± 0.06 percent of the values in the table shown for magnet 2. Magnet 1 requires only a small coil current changes to match magnet 2.

Parameter	Coil M1	Coil M2	Coil E1	Coil C	Coil E2
Coil Start Dimension * (mm)	23.4	464.3	908.7	1056.7	2408.7
Coil Length (mm)	201.2	199.5	110.6	1314.3	110.6
Coil Inner Radius (mm)	258.0	258.0	258.0	258.0	258.0
Coil Thickness (mm)	46.2	30.9	60.9	22.1	67.8
Number of Turns in the Coil	4830	3192	3584	15360	3968
Maximum Coil Design Current I_D ** (A)	264.8	285.6 [^]	233.7 [^]	275.5	240.2
Coil or Coil Set Self Inductance (H)	~ 12.0	~ 5.0		~ 74.0	
Coil or Coil Set Stored energy at I_D (MJ)	0.42	0.20		~ 2.80	
Magnet Cold Bore Diameter (mm)			490		
Cold Mass Outer Diameter (mm)			~ 690		
Cold Mass Length (mm)			2544		
Shield Average Diameter (mm)			~ 1100		
Magnet Warm Bore Inner Diameter (mm)			~ 403		
Magnet Cryostat Outer Diameter (mm)			~ 1400		
Magnet Cryostat Length (mm)			~ 2730		

* The zero point is the match coil end of the cold mass

** The design current is based on a muon beam momentum of 240 MeV/c with the focusing coils in the cusp mode.

[^] These two currents can be adjusted to reduce the current in M2 and get maximum field uniformity in the three-coil set.

The original magnet thermal shield was a 6061-T6 aluminum cylinder that ~ 6.4 mm thick, ~ 2.65 m long and ~ 1.1 m diameter. The shield has 6061-Al end plates and a 6061-Al inner shield that is ~ 0.45 m in diameter. Because the original shield was fabricated from 6061 aluminum it wasn't necessary to sub-divide the shield to prevent the interaction of shield eddy currents with the magnetic field during a quench.

The coolers are mounted so that they can be dropped into the cryostat [9]. This permits the coolers to be shipped separately from the magnet. The cooler is mounted in a sleeve with a tapered copper ring into which the cooler first stage is connected. The sleeve from the room temperature top plate to the surface of the liquid helium is filled with helium gas. The condenser mounted on the second stage re-condenses helium boiled in the cold mass vessel. There is a heat leak of ~ 3 W per cooler from room temperature to the first-stage. The effective first-stage cooling at 40 K per cooler is ~ 37 W. The temperature drop across the connection between the cooler first stage and the copper plate the HTS leads and the shield is attached is ~ 1 K when 40 W is transferred across the joint. There is a heat leak down the sleeve from the cooler first stage to the cooler second stage is ~ 0.25 W. Thus the effective cooling per cooler available at 4.2 K is ~ 1.25 W. If the second stage temperature is raised to 4.6 K (the helium pressure in the cryostat is ~ 0.142 MPa) the effective cooling per cooler available on the second stage is increased to ~ 1.65 W.

The tests described in this report were on magnet 2. During tests of magnet 2 in 2009 (Case 2A in TABLE 2), the end shield temperature was never < 106 K, which meant the cold mass support thermal intercepts were at temperatures > 106 K. The shield was cooled using liquid nitrogen as well as the cooler first stages. The first stage temperatures for the three coolers were between 66 and 74 K with no current in the magnet. The copper plate temperature near the lead farthest from the coolers was 81 K with no magnet current. This temperature rose to 93 K when 239 A was in all five coils. At this point the HTS lead farthest from the coolers failed [10]. The magnet quenched safely because of six of the nine diode packs and their resistors protected all of the magnet coils [7].

In late 2009, the turret was modified to bring down the temperature of the tops of the HTS leads. A single stage Cryomech AL-330 GM cooler was added. This cooler generates 140 W at 40 K [11]. Each of the two-stage pulse tube coolers generates 40 W at 40 K while generating 1.5 W at 4.2 K [12]. In addition the copper leads between room temperature and the tops of the HTS were changed to reduce the lead heat leak from ~ 145 W to ~ 105 W at full current [13]. When the magnet was tested in March of 2010 (Case 2B in TABLE 2), the cooler first stages and the copper plate the HTS leads were thermally connected to, operate at temperatures between 43 and 49 K [14]. The HTS leads tops were between 48 and 51 K. There was no liquid nitrogen cooling on the shield. The temperature of the coldest part of the shield was ~ 72 K. The ends of the shield where the cold mass supports connect to the shield were at a temperature that was between 84 K and 97 K, which was still too high by 30 degrees.

The LBL engineers decided that the excess cooling at 4.2 K should be >1 W. One can't reduce the excess heating in the magnet by 2.5 W without making changes to the magnet cryostat. The changes included; 1) changing the shield material from 6061-T6 aluminum to annealed 1100-O aluminum, 2) greatly reducing the thermal resistance between the cooler first stages and the shield by changing the materials in the interconnects, 3) improving the connection between the shield and the magnet cold mass support intercepts. 4) increasing the number of PT415 two-stage coolers from three to five, and 5) changing the MLI around the magnet cold mass and shield. All of these changes were done on magnet 2 and later on magnet 1.

SHIELD CHANGES AND COOLER TO SHIELD CONNECTION CHANGES

The changes that can have the largest changes in the performance of the cryogenic system are changes in the shield and changes in the connection between the copper plate in the turret and the shield. The two stage coolers and the single stage cooler cool the copper plate that the tops of the HTS leads are attached to. The GM cooler could not be attached to the magnet shield. Attaching the single stage cooler directly to the shield would make the maintenance of that cooler more difficult. All of the coolers are located in the magnet turret. Changing the shield and the connection between the copper plate in the turret and the shield required that the magnet cryostat be completely reassembled. The magnet vacuum vessel and the turret had to be modified in order for two more two-stage coolers to be added. The additional coolers were to be connected to the cold mass at its ends. The three original two-stage coolers were not moved. The single stage cooler position was changed so it could cool the copper plate along with the five two-stage coolers. The HTS leads are located so that the temperature of the tops of the leads is minimized. Figure 1 shows simplified thermal network diagrams comparing the magnet cryogenic system tested in winter of 2010 (Case 2B) with the system tested in the fall 2012 and the winter of 2013 (Case 2C).

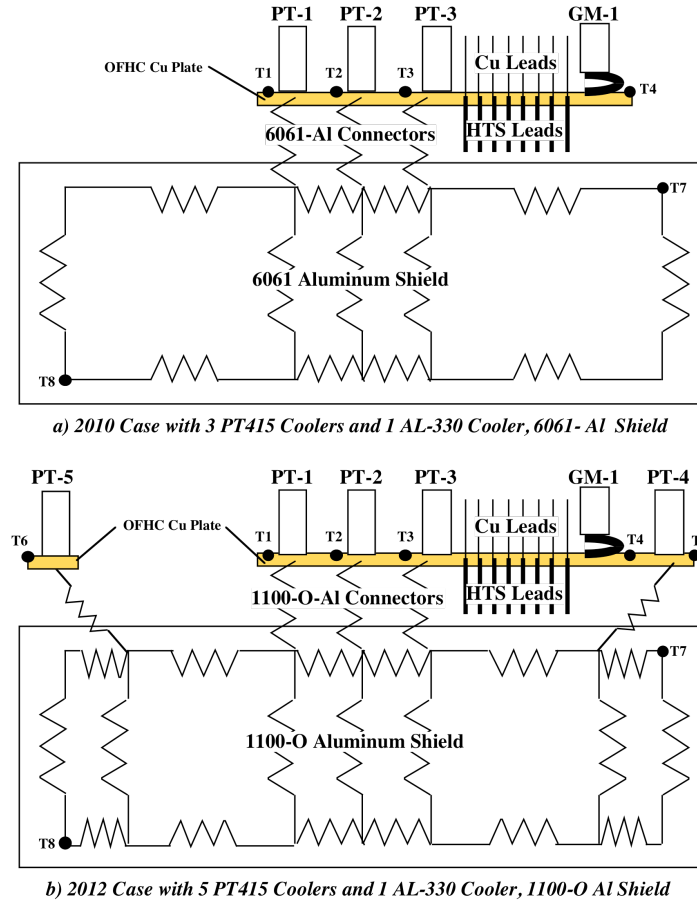


FIGURE 1. Thermal Network diagrams for a 2.7-m long Magnet (Magnet 2) tested in 2010 (Case 2B) and 2012-13 (Case 2C). Temperature sensors T1 through T8 are the location of some of the shield and copper plate sensors. Sensors T1 through T6 are not located on the first stages of the coolers. These sensors are in the OFHC copper plate. They are not found in TABLE 2.

The 2010 system consisted of three two-stage coolers with first-stages that connect to the center of the 6061-T4 aluminum shield. The HTS leads were connected to a copper plate that is between the single stage cooler, which is connected only to the copper plate, and the three two-stage coolers, which are connected to the copper plate and the shield [14]. The 2012 configuration has the three original cooler first stages connected to the center of an 1100-O aluminum shield. The first-stages of two other two-stage coolers are attached to the upper ends of the 1100-O aluminum shield. The single stage cooler is attached to the copper plate near the tops of the HTS leads. The 2012 configuration has five cooler first stages connected to the copper plate and the top of the shield along its length. A general expression for the thermal resistances shown in Fig. 1 can be estimated using the following [15];

$$R = \frac{L}{k(T_{AVE})A_C}, \text{ and} \quad (1)$$

$$\Delta T = RQ, \quad (2)$$

where ΔT is the temperature drop across a node; Q is the heat flowing through the resistance R between nodes. L is the length of the path between the nodes; A_C is the cross-section area of the path between nodes; and the $k(T_{AVE})$ is the thermal conductivity (at an average temperature T_{AVE}) of the material between the nodes. At each node there is a heat load that goes into that node. In order to reduce the shield temperature for a given copper plate temperature, one must reduce the heat input into the nodes (reducing the heat input per unit area into the shield), increase the number of nodes that feed heat into the copper plate (in this case from 3 nodes to 5), and increase the thermal conductivity of the material between the nodes. In general the cross-section area of the material was not changed. The system with five cooler first-stages connected to the shield spreads the refrigeration and thus reduces the ΔT . The most important thing is increasing the thermal conductivity of the material in the shield and in the connectors that carry the heat from the shield to the copper plate which is at ~ 45 K. The networks shown in Fig.1 can be solved like electrical networks or the problem can be solved with ANSYS.

6061-aluminum is a material that has a low RRR (typically between 1.5 and 2.5 depending on the temper). At temperatures below 140 to 200 K, the resistivity of 6061-aluminum is at its minimum value [16]. In the region between 40 K and 100 K, the thermal conductivity of 6061-aluminum goes down almost linearly with temperature. Annealed 1100-O aluminum has an RRR between 14 and 32 (typically about 25) [16]. The resistivity of 1100-O aluminum reaches a minimum at ~ 30 K. From 40 K to 100 K, 1100-O aluminum thermal conductivity goes up as the temperature goes down. At 100 K, the thermal conductivity of 1100-aluminum is 3.5 times that of 6061-aluminum. At 40 K, the thermal conductivity of 1100-aluminum is ~ 14 times that of 6061-aluminum. The shield temperature is closer to 40 K when the shield and connectors are made from 1100-O aluminum. The temperature at the places where the cold mass support intercepts connect to the shield can be up to a factor of two lower when the 1100-O shield and connectors are used. The shield temperature has a direct correlation with the heat flow into the cold mass. The heat flow into the cold mass varies as the intercept temperature to about the 1.8-power when oriented glass-fiber epoxy supports are used in the cold mass supports [17].

The thermal shield around the cold mass had to be redesigned to reduce the eddy current within the shield during a magnet quench. The average electrical resistivity of the shield is reduced from $\sim 1.8 \times 10^{-8}$ ohm-m for a 6061 shield to $\sim 1.5 \times 10^{-9}$ ohm-m for an annealed 1100-O shield at 50 K. This has led to having a shield that is subdivided to break up the eddy currents induced in the shield, when the magnet quenches [18].

OTHER CHANGES THAT AFFECT HEAT FLOW TO THE COLD MASS

While the shield material and the connections from the shield to the coolers were changed, changes in the MLI around the cold mass support eliminated a potential source of thermal shine from 300 K directly to the 4 K cold mass. It is good practice to cover the cold mass support on the low temperature side of the cold mass support. This was not done on this magnet because there wasn't room for a shield and the cold mass support within the 150 mm diameter tube that carries the warm of the cold mass support beyond 1400 mm diameter magnet vacuum vessel.

The change in the MLI and the magnet vacuum system were potentially important. The importance the MLI is difficult to quantify. The effects of bad vacuum become quite apparent quickly. The heat leaks through MLI is greatly affected by the technique used to apply the MLI and whether there are any holes in the MLI that can lead to shine from a higher temperature. The area of the cryostat vacuum vessel and the turret vacuum vessel is ~ 18.6 m². The area of the thermal shield is 16 m². The area of the 4 K cold mass is ~ 11 m². Given the area of the shield and the cold mass, it is clear that errors in applying the MLI can result in additional heat loads that are not well

understood. A reduction of the shield temperature a factor of two can reduce the radiation and conduction heat load by a factor of three or more. The original calculated heat flow to the copper plate from the leads, cold mass supports, thermal radiation and conduction was ~150 W of which the leads represented 109 W [19]. The measured heat load to the first stages of the coolers in March of 2010 was 277 W without current in the leads and 308 W with a current of 250 A in the six 500-A leads. There was a lot of room for improvement in the heat load to the magnet shield. The MLI blankets were carefully fitted to the cold mass and the shield such that the MLI is uncompressed and so that there are no gaps in the MLI. The vacuum was monitored with a high vacuum gauge capable of measuring pressures <0.0133 mPa ($<10^{-7}$ torr). In 2012, when the magnet is cold, the measured vacuum in the cryostat vacuum vessel was from 0.001 to 0.01 mPa (without current in the coils). Since the vacuum pressure gauge is magnetic field sensitive, an accurate measurement of the vacuum was not possible when the magnet was powered.

Only some of the tubes entering the magnet were properly staged to the first stages of the coolers. The main vent pipe and fill pipes weren't properly staged to the cooler first stage, because of their locations. In order to properly stage all of the tubes, a larger magnet turret had to be built. The instrumentation wiring was changed to low heat leak wires. Some of these wires could be staged to the cooler first stages. The rest could not be staged to the copper plate. In general, the instrumentation wiring doesn't carry more than 10 μ A of current and many wires carry no current at all. There wasn't much to be gained by trying to stage all of the instrumentation wires to the cooler first-stages. All of the temperature sensors are calibrated CERNOX mounted on buttons so that the sensor wires will be at the same temperature as the place where the temperature is measured. The temperature sensor button can be screwed and glued to the place where the temperature is being measured. As a result, far fewer temperature sensors will fail.

Changing the number of two stage coolers from three PT415 coolers to five PT415 coolers is a brute force approach to solving the problem of inadequate 4 K cooling. Spreading the two stage coolers along the top of the shield reduces the ΔT in the shield, but this effect was probably minor compared to changing the shield material and reducing the thermal resistance of the shield connector to the copper plate. Increasing the number of coolers is as large an effect on the magnet cooling as the changes in the shield and shield connection to the copper plate.

A COMPARISON OF 2012 AND 2013 MEASURED DATA WITH EARLIER DATA

TABLE 2 compares the measured temperatures on magnet 2 in various places on the magnet for six different cases at various times from July 2009 to May of 2013. The six cases are as follows: 1) Case 2A was for magnet 2 as tested in the summer of 2009 (with no current). The magnet was not kept cold using three PT415 two stage coolers. The copper leads from 300 K were not optimum. The heat leak with no current was too low, but the lead heating at full current was too high [13]. The first stages of the three two-stage coolers cooled the shield and the leads. In addition the shield was cooled using liquid nitrogen in a place near where the shield was connected to the coolers. 2) Cases 2B-1 and 2B-2 were for the magnet 2 as it was tested in March of 2010. The shield is the same 6061-Al shield as used in case 2A. The connections from the coolers to the shield were the same as in case 2A. A single stage AL330 GM cooler was attached to the copper plate at the end opposite from the PT415 coolers [20]. The copper leads from room temperature were optimized to reduce the heat load when they carried the full design current of 275 A [20]. The first stages of the three PT415 two-stage coolers and the AL330 single-stage cooler cooled the shield and the leads. There was no liquid nitrogen shield cooling. 3) Case 2B-2 is the same configuration as Test 2B-1 except the six large HTS leads carry 250 A. 4) Case 2C-1 was for the magnet as it was tested in the fall of 2012. All of the improvements described in the previous two sections were made. The shield and leads were cooled using five PT415 two-stage coolers and one AL-330 single stage cooler. This test was done with no lead current. 5) Case 2C-2 is the same as case 2C-1. The leads carry their full design currents. In terms of lead heating this case is equivalent to Case 2B-2 where six HTS leads carry a current of 250 A. 6) Case 2C-3 was for the same magnet configuration as case 2C-1. Two PT415 coolers (coolers PT-1 and PT-5) were shut off. The two coolers that were not operating added to the heat leak to the first-stages of the four remaining coolers (PT-2, PT-3, PT-4, and GM-1) that were operating.

The measured data included in TABLE 2 is the first-stage temperatures of the five PT415 coolers (PT-1 through PT-5) and the AL330 cooler (GM-1). The copper plate temperature near the leads (sensor T4) is included. The shield temperature on the upper shield at one end (sensor T7), the lower shield at the other end (sensor T8), and the shield in the magnet bore are also included. The measured temperature at the bottom of the helium tank at one end is included. The measured temperature in the helium tank at the top on the opposite end is also included. (In some cases the temperature sensor at the top of the helium tank was in helium gas.) The helium pressure in the tank is included to correlate with the measured temperatures. In case 2A, the heat removed by the liquid nitrogen was included; in all the other cases there was no liquid nitrogen cooling. The amount of calculated cooling generated by

the PT415 cooler first-stages as a function of temperature and second-stage heat load is based on measurements of a PT415 cooler taken at Florida State University [21]. Cooling generated by the AL330 single stage GM cooler is based on measured Cryomech data [11]. This data was curve fitted [14]. From the measured first stage temperatures, an estimate of the total heat load to the shield and the copper plate was made. The total available cooling at 4.35 K is given. The excess 4.35 K cooling is estimated for the cases shown in TABLE 2.

TABLE 2. A Comparison between various Test Cases from 2009, 2010, 2012 and 2013 (The comparison includes the total available cooling at 4.35 K, and the excess cooling. If the excess cooling is positive, the magnet is kept cold with the coolers. If the excess cooling is negative liquid helium is boiled away at the rate of 1.48 L hr⁻¹ per W at 4.35 K.)

Parameter	Case 2A	Case 2B-1	Case 2B-2	Case 2C-1	Case 2C-2	Case 2C-3
Number of Coolers	3	4	4	6	6	4
Magnet Current (A)	0	0	250	0	Design*	0
1 st Stage T Cooler PT-1 (K)	65.6	44.0	45.1	35	40	59.4***
1 st Stage T Cooler PT-2 (K)	~70*	~43.2**	~45.3**	38	41	51.2
1 st Stage T Cooler PT-3 (K)	74.2	42.7	45.6	38	42	50.9
AL330 T Cooler GM-1 [#] (K)	No Cooler	42.0	46.2	21	23.6	26.3
1 st Stage T Cooler PT-4 (K)	No Cooler	No Cooler	No Cooler	40	44	50.3
1 st Stage T Cooler PT-5 (K)	No Cooler	No Cooler	No Cooler	33	39	86.9 ***
Cu Plate at Leads Temp T4 (K)	80.9	~48.2	50.5	48.5	51.0	60.6
Shield Top Temp T7 (K)	106.5	~88.1	~87.2	~41	48.3	59.1
Shield Bottom Temp T8 (K)	116.0	~98.6	~98.5	~41	49.0	62.7
Shield Bore Temp (K)	No Data	No Data	No Data	~43	~55	65.5
He Vessel Bottom Temp (K)	4.32	4.26	4.22	4.35	4.22	4.35
He Vessel Top Temp (K)	4.31	4.25	5.14	4.42	4.20	4.37
He Vessel Pressure (MPa)	~0.12	0.102	0.103	~0.12	0.105	1.19
Shield Q to the Coolers (W)	~230	~277	~308	~184	~266	~253
Shield Q to LN ₂ (W)	~32	0	0	0	0	0
Total Shield Heat Load (W)	~262 [^]	~277 [^]	~308 ^{^^}	~184	~266	~253
Total Cooling at 4.35 K (W)	~2.7	~4.3	~4.2	~7.5	~7.3	~4.1
Excess Cooling at 4.35 K (W)	<-3.0 ^{^^^}	-1.4	-1.5	~5.0	~4.8	~1.3

* All eight leads carry their full design current. In terms of the Cu lead heating this is equivalent to the currents to case 2B-2.

** This sensor was not operating. This is an estimate of the first stage temperature based on the adjacent Cu plate temperature.

*** This cooler is shut off, so the cooler first stage temperature is higher than the other coolers that are operating. Note the first-stage of PT-5 is not connected to the copper plate, to which the first-stages of all the other coolers are connected.

[#] There is a copper strap between sensor T4 and the GM-1 cooler first stage. The ΔT between sensor T4 and the GM-1 cooler first stage can be larger than the ΔT the other sensors and the nearby cooler first stages.

[^] The copper leads were not optimum. The copper lead heat leak with no current was ~28 W. At full current the copper lead heat leak was about ~140 W. The leads for case 2B-1 have a zero current heat leak of about 54 W. At full current the copper lead heat leak is about 105 W. At full current, the first stage heating for case 2A would be more than for case 2B.

^{^^} The heating in this case had not yet reached equilibrium because the time was too short. The expected heating was ~315 W.

^{^^^} Because of high first stage temperatures, the cooler second stage cooling is ~1 W instead of ~1.5 W. Thus the excess cooling is more negative than for cases 2B-1 and 2B-2.

The magnet in tests 2C was allowed to operate with the helium pressure in the tank negative relative to the atmospheric pressure at an elevation of ~100 m. The minimum pressure measured was 0.04 MPa (0.4 bar) absolute. This corresponds to an average second-stage temperature for the five PT415 coolers of 3.4 K. (Note: the cooler second stage temperature fluctuates about 0.3 K at 4.2 K at a frequency of 1.2 Hz. The average second stage temperature is determined from the magnet cryostat pressure. It appears that the magnet can operate in a stable way with about 2.5 W of cooling at 4 K. At 4.25 K, the five PT415 coolers will produce ~7.5 W of cooling given the heat load to the cooler first-stages. Since it is desirable to maintain a pressure above atmosphere in the helium vessel, the excess cooling in cases 2C-1 through 2C-3 was taken up by adding heat to the cold mass using a heater that is controlled by a proportional controller.

AN ANALYSIS OF THE MEASURED DATA

Two things are absolutely clear from the measured data. The static heating (at zero current) to the shield, the copper plates and thus first stages of the coolers was reduced by a factor of ~ 1.5 as compared to the magnet in cases 2A or 2B. (Case 2A and 2B magnet had the same shields, the same heat transfer elements from the shield to the first stages of the two stage coolers, and the same MLI around the shield and the cold mass support intercepts.) In case 2C-2 (with the design current running in all of the magnet coils), the lead heat load represents over half of the 266 W heat load to the shield and the copper plates connected to the cooler first stages. The heat load to the cold mass was reduced from ~ 6 W to ~ 2.5 W, when one compares cases 2B-1 and 2C-1.

A key factor in the reduction of the heat load to the cold mass was the reduction of the shield and cold mass support intercept temperatures. The shield temperatures were reduced by over a factor of two. The temperature distribution within the shield was far more uniform in case 2C than it was in either case 2A or case 2B. The shield material change from 6061-T4 aluminum to 1100-O aluminum is a major contributing factor to the uniformity of the shield temperatures. An improvement of the MLI around the shield and the cold mass supports was a contributor to the reduction of the static heat load (at zero current) to the magnet shield in the 2C cases. The two added coolers PT-4 and PT-5 contributed 85 W of the 266 W cooling provided to the shields in case 2C-2. Without coolers PT-4 and PT-5, the shield temperature would have increased to over 60 K at the ends. The shield temperature within the magnet bore would be about 65 K given the improvements of the MLI and the change in the shield material from 6061 aluminum to 1100 aluminum. The improvement of the connection between the two-stage cooler first stages and the shield is also a strong contributing factor to the lower shield temperature.

The contribution of the single stage cooler to the total shield cooling is smaller in case 2C-2 as compared to case 2B-2. In case 2B-2 the single stage cooler GM-1 produced 157 W of the 308 W of first stage cooling. In case 2C-2, the single stage cooler produced 58 W of the 266 W of first stage cooling. The reduced contribution of the single stage cooler in cases 2C-1 and 2C-2 may be due to a higher thermal resistance connection between the copper plate to the single stage cooler than in cases 2B-1 and 2B-2. In cases 2C-1 and 2C-2, the temperature of the cold head of the single stage cooler was much lower than the first stages of the two stage coolers connected to the copper plate. In cases 2B-1 and 2B-2, the single stage cooler cold head temperature was much closer to the first stage temperatures of the two stage coolers that were all connected to the copper plate.

Case 2C-3 came about because the magnet doesn't stay trained after it has been warmed to room temperature. The magnet can be kept cold and full of liquid helium with three of the five two-stage coolers running. The two-stage coolers not running contribute to the heating of the shield and the copper plate because heat is conducted to the first stage from the room temperature end of the cooler. Because the first stage temperature is higher in case 2C-3 than in cases 2C-1 and 2C-2, there is an increase in the heat leak to the cold mass. Because there is stratification in the gas below the condensers of the two shut-off coolers, the added heat to the cold mass from the shut off coolers is not over 0.5 W. It does not appear that one can shut off a third two-stage cooler and keep the liquid helium in the magnet cryostat. When one compares cases 2C-1 and 2C-3, one sees that the two coolers that are shut off contribute ~ 79 W to the shield heating. The two coolers that were shut off contribute ~ 0.6 W of additional heating at 4.3 K.

CONCLUDING COMMENTS

When any magnet is cooled using two stage coolers, one must pay close attention to the details. The tops of the HTS leads must operate at a temperature that is < 50 K. Changing the shield material to 1100-O improved the temperature uniformity within the shield. Improving the connection between the cooler first-stages reduced the shield temperature to a range between 41 K to 55 K depending on the location on the shield and the total heat load onto the cooler first stages. The colder shield reduces the cold mass support heat flow and the radiation heat flow to the cold mass. Changing the shield and the shield connection to the coolers reduced the 4 K heat load by > 2.5 W.

Adding two more two-stage coolers increased the cooling margin by ~ 2.5 W. The ability to keep the magnet temperature at 4 K with one or more coolers shut off is of interest, because one does not have to retrain the magnet if it is kept cold (say < 50 K). Keeping the magnet cryostat full of liquid helium is desirable during a short shut down. If the magnet shutdown is longer, it appears that the magnet can be kept cold at ~ 50 K with as few as two coolers.

When the tops of the HTS leads are kept cold, there is more temperature margin in the leads. The extra margin is especially necessary when the HTS leads are in a magnetic field [22]. In magnets with high inductances, one can't discharge the magnet rapidly without quenching the magnet. Magnet quenching should be avoided, because cooling a magnet back down with liquid helium is not always easy when helium is in short supply.

ACKNOWLEDGMENTS

The authors acknowledge the efforts of many who helped with the testing of the magnet. A partial list includes: S. Griffiths, I. Mullacrane, and A. Oates from Daresbury; P. Hanlet, R. Pilipenko, L. Coney, and M. Leonova from Fermilab; T. Luo, A. DeMello, A. Lambert, N. Y. Li, and E. Rochepault from LBNL and others behind the scenes.

This work was supported by the Office of Science of the United States Department of Energy under DOE contract DE-AC-02-05CH11231.

REFERENCES

1. P. Fabricatore, S. Farinon, U. Bravar, and M. A. Green, "The Mechanical and Thermal Design of the MICE Detector Solenoid Magnet System," *IEEE Transactions on Applied Superconductivity* **15**, No. 2, pp 1255-1258, (2005).
2. M. A. Green, C. Y. Chen, T. Juang et al, "Design Parameters for the MICE Tracker Solenoid," *IEEE Transactions on Applied Superconductivity* **17**, No. 2, pp1247-1250, (2007).
3. S. Q. Yang, M. A. Green, G. Barr, et al, "The Mechanical and Thermal Design for the MICE Focusing Magnet System," *IEEE Transactions on Applied Superconductivity* **15**, No. 2, pp 1259-1262, (2005).
4. HTS-110 Ltd. Lead specifications for 100 A HTS leads and 500 A HTS leads, HTS-110 Gracefield Research Center, 69 Gracefield Road, Lower Hutt 5010, New Zealand, www.hts110.co.nz/current-leads/ (2013).
5. M. A. Green and S. P. Virostek, "The Dimensions and Number of Turns for the Spectrometer Solenoid as built compared to the Original Magnet Design," MICE Note 207, www.MICE.itt.edu, (June 2008)
6. X. L. Guo, M. A. Green, L. Wang, H. Pan, and H. Wu, "The Role of Quench-back in the Passive Quench Protection of Long Solenoids with Coil Sub-division," *IEEE Transactions on Applied Superconductivity* **20**, No. 3, pp 2035-2038, (2010).
7. M. A. Green, H. Pan, S. O. Prestemon, and S. P. Virostek, "Protecting the Leads of a Powered Magnet that is protected with Diodes and Resistors," *IEEE Transactions on Applied Superconductivity* **22**, No. 3, pp 4702204-2207, (2012).
8. S. P. Virostek, et al, "Update on the Modification and Testing of the MICE Superconducting Spectrometer Solenoids," *Proceedings of PAC-2011*, New York NY (2011).
9. M. A. Green and S. T. Wang, "Tests of Four PT415 Coolers Installed in the Drop-in Mode," *Proceedings of the International Cryogenic Engineering Conference 22*, Seoul Korea, 21-25 July, p 105, 2008.
10. S. P. Virostek, M. A. Green, F. Trillaud and M. S. Zisman, "Fabrication, Testing and Modeling of the MICE Spectrometer Superconducting Solenoids," *Proceedings of IPAC-10*, Kyoto Japan, pp 409-411, (2010).
11. AL330 Cooler Specification and Data Sheets, Cryomech Inc., 113 Falso Drive, Syracuse NY 11321, www.Cryomech.com.
12. PT415 Cooler Specification and Data Sheets, Cryomech Inc., 113 Falso Drive, Syracuse NY 11321, www.Cryomech.com.
13. M. A. Green and S. T. Wang, "Test of Copper and HTS Current Leads with a Two-Stage Drop-in Cooler," *Advances in Cryogenic Engineering* **57**, pp 581 - 589, AIP Press, Melville NY (2012).
14. M. A. Green, "What Happened to Spectrometer Magnet 2B?" MICE Note 292, www.MICE.itt.edu, (May 2010).
15. M. A. Green and S. Q. Yang, "Heat Transfer into and within the 4.4 K Region and the 40 K Shields of the MICE Focusing and Coupling Magnets," MICE Note 101, www.MICE.itt.edu, (April 2004).
16. *Handbook of Materials for Superconducting Machinery*, Metal and Ceramics Information Center, MIC-MB-04, National Bureau of Standards, Boulder CO, (January 1977) data on 6061 and 1100-O aluminums.
17. M. A. Green and S. S. Chouhan, "The Cyclotron Gas-stopper Magnet Shield, should it be cooled with Liquid Nitrogen or should it be cooled by the Coolers?" MSU FRIB Note FRIB-M40201-CA-000108, (May 2013).
18. H. Pan, S. O. Prestemon, S. Virostek, et al, "Eddy-currents and the Force Analysis for the Thermal Shields of a Superconducting Solenoid with Separately Powered Coils," MICE Note 420, www.MICE.itt.edu, (October 2012).
19. M. A. Green, L. Wang, H. Pan, H. Wu, et al, "Lessons Learned for the MICE Coupling Solenoid from the MICE Spectrometer Solenoid," *Proceedings of IPAC-10*, Kyoto Japan, May 2010, pp 406-408, (2010).
20. M. A. Green and S. P. Virostek, "Using a Single-stage GM Cooler to Augment the Cooling of the Shields and Leads of a Magnet Cooled with Two-stage Coolers," *Advances in Cryogenic Engineering* **57**, pp 589-596, AIP Press, Melville NY (2012).
21. Y. S. Choi, T. A. Painter, D. L. Kim, et al, "Helium-Liquefaction by Cryocoolers for High-Field Magnet Cooling," *Proceedings of the International Cryocooler Conference* (2006).
22. M. A. Green and H. Witte, "Using High Temperature Superconducting Leads in a Magnetic Field," *Advances in Cryogenic Engineering* **53**, pp 1251-1258, AIP Press, Melville NY (2008).

DISCLAIMER

This document was prepared as an account of work sponsored by the United States Government. While this document is believed to contain correct information, neither the United States Government nor any agency thereof, nor The Regents of the University of California, nor any of their employees, makes any warranty, express or implied, or assumes any legal responsibility for the accuracy, completeness, or usefulness of any information, apparatus, product, or process disclosed, or represents that its use would not infringe privately owned rights. Reference herein to any specific commercial product, process, or service by its trade name, trademark, manufacturer, or otherwise, does not necessarily constitute or imply its endorsement, recommendation, or favoring by the United States Government or any agency thereof, or The Regents of the University of California. The views and opinions of authors expressed herein do not necessarily state or reflect those of the United States Government or any agency thereof, or The Regents of the University of California.